

Synthesis of 4, 4'-Stilbene Dicarboxylic Acid and Aniline Modified Graphene Oxide and Its Electrochemical Performance for Supercapacitors

Asim Riaz, Adil Usman, Zakir Hussain *

School of Chemical and Materials Engineering (SCME), National University of Sciences & Technology (NUST), Sector H-12, 44000 Islamabad, Pakistan

Tel.: 0092 51 9085 5205; Fax. 0092 51 9085 5002

*E-mail: zakir.hussain@scme.nust.edu.pk

Received: 26 October 2015 / Accepted: 19 November 2015 / Published: 1 January 2016

Graphene oxide obtained through liquid ex-foliation of graphite flakes by improved Hammer's method have been functionalized with stilbene-4, 4'-dicarboxylic acid and aniline and electrochemical performance of covalently functionalized graphene oxide was investigated. All samples were characterized through FTIR, XRD, FESEM, UV-Vis and electrochemical performance was measured through cyclic voltammetry (CV) analyzer. High level of oxidation was observed in graphene oxide and 002 plane of graphene oxide was confirmed at 10.3° . It was found that with the functionalization of graphene oxide, the capacitance increased up to four and two times for stilbene-4, 4'-dicarboxylic acid and aniline modified graphene oxide respectively. The optical absorption was red shifted as high as 104 nm wavelength, showing higher conjugation effect in stilbene-4, 4'-dicarboxylic acid modified graphene oxide as compared to 45 nm in the case of aniline modified graphene oxide.

Keywords: Stilbene 4, 4'-dicarboxylic acid, Esterification, Capacitance, Graphene oxide

1. INTRODUCTION

The research interest in energy field is increasing dramatically due to the need of efficient energy production and better performing energy storage devices which can be fabricated with green technology with low harmful emissions [1]. Supercapacitors are thought to be future energy storage devices due to their added advantages over conventional secondary batteries e.g. high charge density, no toxic emissions and most importantly their superior charge/discharge characteristics. A lot of research has been carried out for high performance supercapacitors electrode materials which possess excellent electrical conductivity and high capacitance.

Carbon based materials e.g. carbon nanotubes (CNTs), carbon fibers, carbon aerogel and activated carbon are commonly used electrode materials for supercapacitors. In the last few years, graphene has got lot of attention as electrode material for supercapacitors [2]. Two dimensional graphene is an allotrope of carbon having thickness of one carbon atom with 0.142nm C-C bond length [3]. Large surface area [4], high electrical/thermal conductivity [5], high charge mobility [6, 7], outstanding optical transmittance, excellent mechanical strength [8] and thermal stability of graphene makes it highly suitable for batteries, solar cells, light emitting diodes (LEDs), sensors, supercapacitors, transparent electrodes, actuators and field effect transistors (FETs) etc. [9-16]. The extraordinary electrical properties in graphene are due to the fact that electron transfer inside graphene is like a wave because of enhanced delocalization present in its electronic structure [17, 18]. Additionally, easy dispersibility of graphene and its transparency rendered its use in transparent and flexible conducting electrodes through printing techniques [19].

Graphene oxide (GO) is the oxidized form of graphene, which can easily be dispersed in variety of organic solvents and aqueous mediums. Study suggests that water, dimethyl form amide (DMF), *N*-methyl-2-pyrrolidone (NMP) and ethylene glycol are the best mediums for the stable dispersion of graphene oxide [20]. There exist -COOH, -OH and C-O-C groups on the basal planes and edges of GO. The presence of oxygen functionality on the back bone of GO makes it possible to separate the stacked layers with sonication to produce few or mono layered GO [21]. Using graphene oxide in solvent assisted processing techniques for device fabrication, chemical functionalization is always desired in order to get the expected incredible properties of few layered graphene oxide [22]. Scientists have proposed that with the functionalization of GO, it may or may not be completely reduced. If functionalization causes complete reduction of GO, the layers will be stacked due to the removal of oxygen functional groups which can be ex-foliated by sonication due to the π - π electrons repulsion between the sheets. However, in the case of partial reduction, there is a chance to get monolayered GO which possesses electric double layered capacitance having a value of $21\mu\text{F}/\text{cm}^2$ per unit of specific surface area.

Scientists have functionalized graphene oxide with various organic compounds having different functional groups and investigated such materials as supercapacitors electrode material. Partha *et al.* [23] reported the effect of 9-anthracene carboxylic acid on graphene where the capacitance of graphene was enhanced from 110 F/g to 425.8 F/g after modification. The proposed phenomenon for the enhancement of capacitance was the attachment of benzene ring anion to graphene via π - π interactions. In another study, Tae Young *et al.* [24] fabricated high performance supercapacitors in which an ionic liquid modified graphene was used as an electrode along with ionic liquid electrolyte. The capacitance was observed to be 186 F/g.

Based on extraordinary properties of graphene based materials, there is a dire need to further investigate on the potential of chemically modified graphene oxide for its electrochemical performance. In the present contribution, we report on the functionalization of GO with stilbene 4, 4'-dicarboxylic acid and aniline monomer and their optical as well as electrochemical properties. GO was synthesized by improved Hummer's method and subsequently functionalized by standard esterification and amidation process for stilbene and aniline respectively. For the electrochemical performance, double Al electrode assembly was used to prepare the samples and further characterized by CV

analysis. It was noted that with the addition of benzene rings, the electrochemical performance of GO was enhanced.

2. EXPERIMENTAL

2.1. Materials

Graphite Flakes (Graphene Supermarket, USA), Sulphuric Acid (H_2SO_4 , Sigma Aldrich, 98%), Phosphoric Acid (H_3PO_4 , Sigma Aldrich, 98%), Potassium per Manganate (KMnO_4 , Sigma Aldrich, 87%) and Hydrogen per Oxide (H_2O_2 , Sigma Aldrich, 37%) were used for the liquid ex-foliation of graphite flakes to graphene oxide. Stilbene-4, 4'-dicarboxylic acid (Sigma Aldrich, 99%), Aniline monomer (Sigma Aldrich, 99%), Dicyclohexyl carbodiimide (DCC, Sigma Aldrich, 98%) and dimethyl amino pyridine (DMAP, Sigma Aldrich, 98%) were used for the functionalization of GO.

2.2. Liquid Ex-Foliation of Graphite to Graphene Oxide

Improved Hummer's method was used for the synthesis of GO. Briefly, graphite flakes (3.0 g) were poured into the mixture of conc. Sulphuric Acid and Phosphoric Acid and stirred for 30min at room temperature. The ratio of mixture of the acids was 9:1 (360ml: 40ml) for $\text{H}_2\text{SO}_4/\text{H}_3\text{PO}_4$. Further, 18.0g of Potassium per Manganate was added gradually into the mixture which raised the temperature to 40 °C. The slow addition was necessary to avoid harmful effects of exothermic reaction. After 12hrs of stirring at 50 °C, 30% H_2O_2 (3ml) was added and stirred for another 30min. Reaction was quenched by the addition of 400ml crushed ice and the mixture was centrifuged at 4000 rpm for 2 hours to facilitate the ex-foliation process where supernatant was decanted away. Continuing the washing process to achieve neutral pH of the graphene oxide dispersion, the mixture was washed first with 1% HCl in DI water and then with pure DI water repeatedly. After each washing and centrifugation step, supernatant was decanted away and the graphene oxide pellet was re-dispersed in DI water for further centrifugation. Centrifugation time increased from 30 min to 4 hours as pH increased from 2 to 6 due to difficulty of settling graphene oxide layers. Finally, the exfoliated GO was dried at 70 °C in vacuum oven for 48hrs.

2.3. Functionalization of GO with stilbene -4, 4'-dicarboxylic acid (GO-COOH)

GO was modified with stilbene -4, 4'-dicarboxylic acid via esterification of -COOH group of acid and -OH group of GO. In detail, dispersion of GO (0.25mg/ml) was prepared in DMF via sonication for 12hrs and to this dispersion (10mL), 10mM solution of stilbene-4, 4'-dicarboxylic acid in DMF was added. The mixture was kept in an oil bath at 80 °C under stirring for 24hrs. The reaction was catalyzed by the addition of 1.1 g DCC and 100 mg of DMAP under continuous stirring and let it stirred for another 60hrs. Dry N_2 atmosphere was maintained throughout the reaction. Finally, the reaction mixture was brought to room temperature and was centrifuged at 4000rpm for 2hrs. The supernatant was decanted away and the pellet was re-dispersed in methanol and centrifuged again until

clear supernatant was achieved. Drying of the product was done in an oven at 70 °C for 72hrs to obtain gray powder of modified GO.

2.4. Functionalization of GO with Aniline (GO-NH₂)

In this experiment, 200ml GO dispersion (0.5mg/ml) in DMF was sonicated for 8hr to further ex-foliate and to obtain homogeneous dispersion followed by drop wise addition of 0.4ml aniline monomer into the dispersion. The mixture was refluxed at 80 °C for 18hrs under continuous stirring to complete the reaction. The solution was then centrifuged and washed with DMF for the removal of unreacted GO and aniline. The product was dried at 80 °C to obtain black flakes.

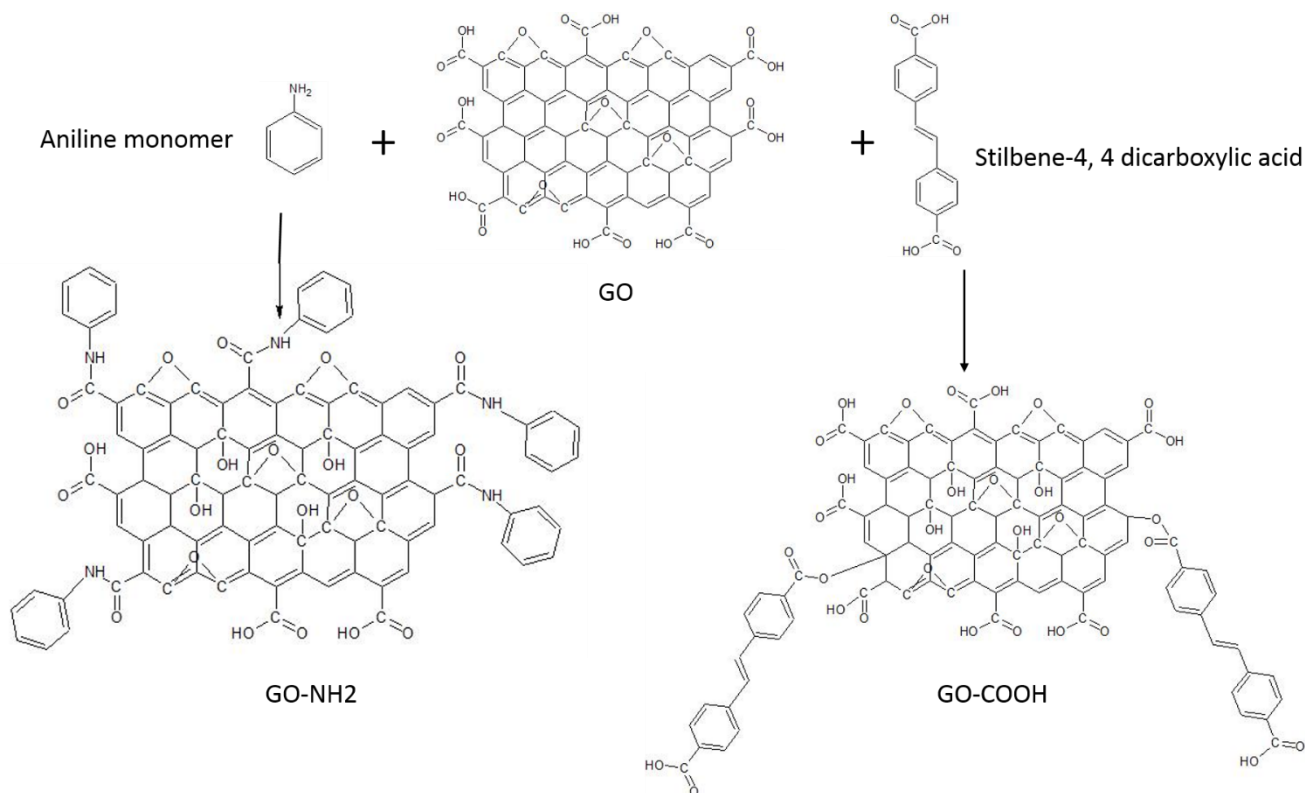


Figure 1. Schematic representation of covalent functionalization of GO with aniline and Stilbene 4,4' dicarboxylic acid showing amide and ester bond formation respectively

2.5. Characterization of Materials

With the help of Field emission scanning electron microscope (MIRA 3-XM manufactured by TESCAN), morphology of GO and modified GO was observed. The dispersion of samples in DMF was drop casted on glass slides. Transmission mode optical microscope was used to visualize the GO sheets, which was spin coated on silicon substrate. X-Rays Diffraction patterns of GO and graphite flakes were acquired by Xpert's PRO PANAnalytical X-Ray Diffractometer (XRD). The machine was equipped with Ni- filtered Cu K α (30kV, 40mA) and the step was 0.020/s. ATR-FTIR (JASCO 7890)

with TGS detector was used to obtain information of various functional groups present in GO as well as in modified GO samples. The samples were analyzed from 400-4000 cm^{-1} with a scan rate of 1cm^{-1} . UV-Vis spectrophotometric analysis of dispersions was carried out by using JASCO 670 from 190 – 1100 nm range in quartz cells (1cm path length). In order to measure the degree of oxidation, CHNSO analyzer (Thermoelectron EA- 1112) was used to measure GO sample where the flow rate for He and Oxygen were set at 140 ml/min and 250 ml/min respectively.

3. RESULTS AND DISCUSSION

Figure 2 shows the FTIR spectra of GO, GO-COOH and GO-NH₂. The characteristic peaks for the graphene oxide such as O-H peak at 3435 cm^{-1} , C-O peak at 1384 cm^{-1} and C=O peak at 1717 cm^{-1} indicated the formation of GO [25]. The C-H bond sp^3 stretching was observed at 2950 cm^{-1} [21, 26]. The presence of hydrogen bonding in the GO molecules was confirmed through the presence of a strong peak of O-H between $3400\text{-}3550\text{ cm}^{-1}$. A sharp peak at 1634 cm^{-1} was observed due to the stretching of C=C bond present in GO [27]. Furthermore, the C-OH groups present on the surface of GO were confirmed by a sharp peak at 1384 cm^{-1} .

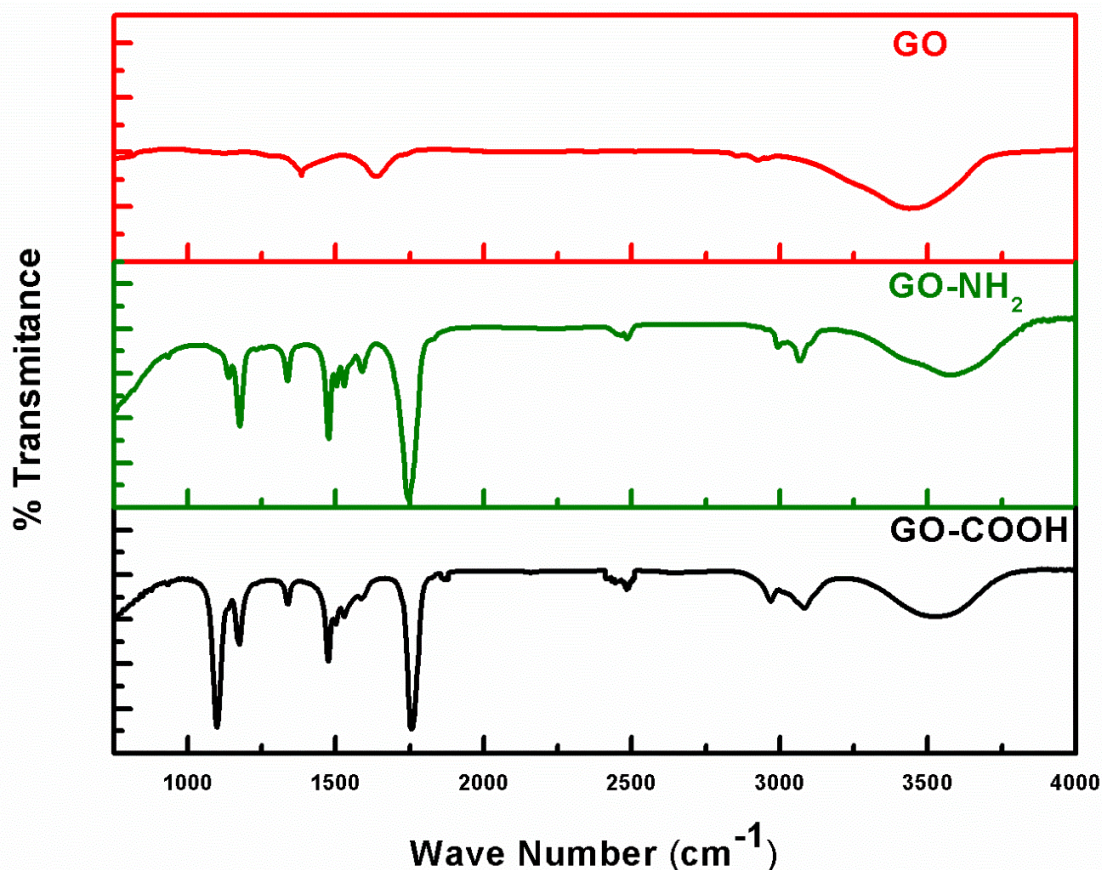


Figure 2. FTIR spectra of graphene oxide (GO) flakes, Aniline functionalized graphene oxide (GO-NH₂) powder and Stilbene 4,4'-dicarboxylic acid functionalized graphene oxide (GO-COOH) powder indicating the characteristics peaks of OH, amide and ester bonds

In the case of modified GO, peak shifting phenomenon was observed due to the incorporation of two new molecules on the basal planes of GO [28]. In the case of GO-COOH, ester carbonyl peak was observed at 1770 cm^{-1} . Similarly, stretching vibrations of the C-O bonds can be observed at 1160 cm^{-1} .

In the case of GO-NH₂, N-H stretching peaks were observed at 3416 cm^{-1} and 3561 cm^{-1} , C=C stretching peak at 1592 cm^{-1} and C-N, C=N stretching peaks at 1305 cm^{-1} and 1320 cm^{-1} respectively [29].

Regarding phase analysis, X-Rays Diffraction analysis of GO and pure graphite flakes was carried out where 002 plane of pure graphite flakes at Bragg's angle of 26.3° with interlayer spacing of 0.34 nm was observed (Figure 3) [21]. In this case the oxidation of graphite flakes into graphene oxide was confirmed from the peak at 10.3° showing 001 plane (Figure 3). In the case of functionalization, the characteristic peak of 001 plane of graphene oxide at 10.3° shifted to 11.5° and 11.1° Bragg's angle in case of GO-COOH and GO-NH₂ respectively. In addition, it was also noted that the intensity of the peak has also been considerably reduced. GO-NH₂ showed two broader peaks around 20° and 30° Bragg's angle which can be attributed to the presence of aniline in the system. In the case of in situ polymerization of aniline to polyaniline, the second peak is observed generally around 25° [30], which was not the case in the present study. While GO-COOH also showed shifting of the peaks in the region of reduced graphene oxide but the presence of peak around 11° indicated the presence of GO, suggesting that the functionalization did not cause complete reduction of graphene oxide.

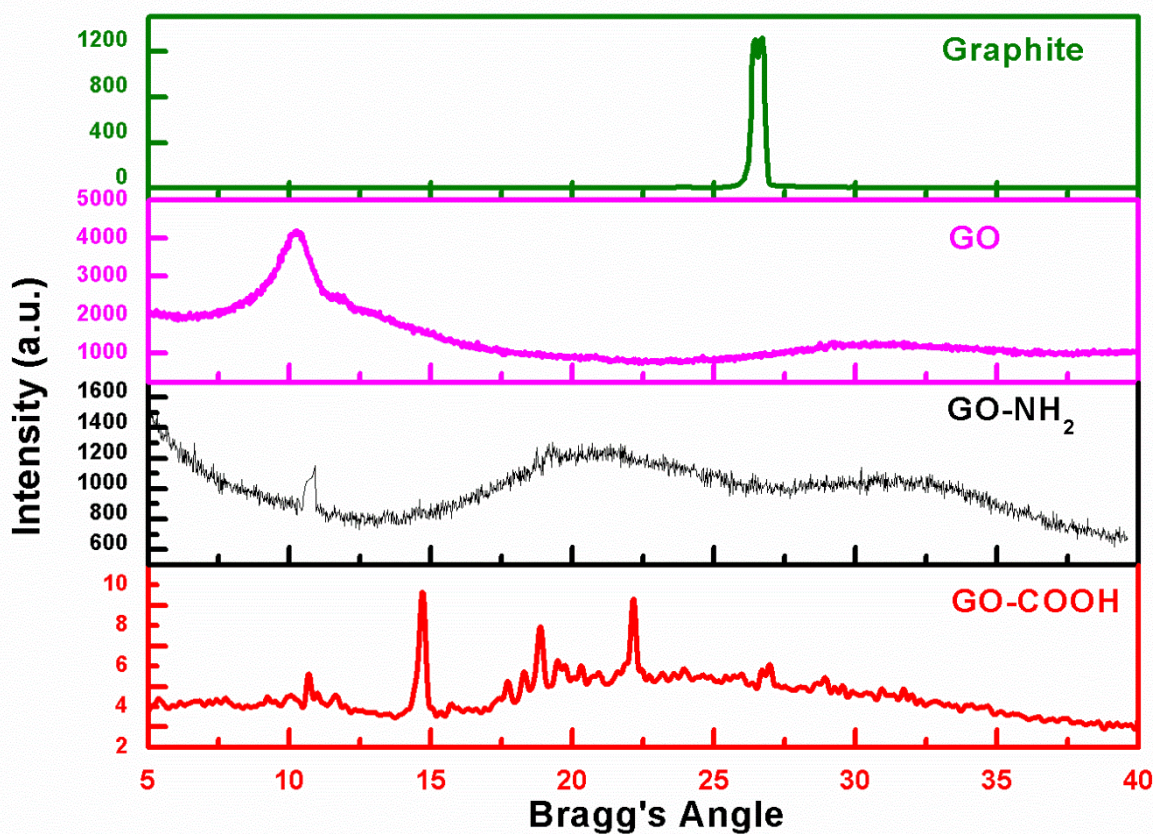


Figure 3. X-Rays Diffraction patterns of Graphite flakes, Graphene oxide and functionalized GO

Topography and surface analysis of GO, GO-COOH and GO-NH₂ was carried out through field emission scanning electron microscopy (FESEM) (Figure 4). Large area continuous sheets of GO can be observed in Figure 4a. The area of GO sheets at 5000 magnification was calculated to be 2000 μm². However, the images of GO-COOH showed the broken transparent GO sheets after acid modification and extensive stirring at 80 °C during reaction (Figure 4c). In the case of GO-NH₂ the modified sheets appeared to be continuous as compared to GO-COOH (Figure 4b).

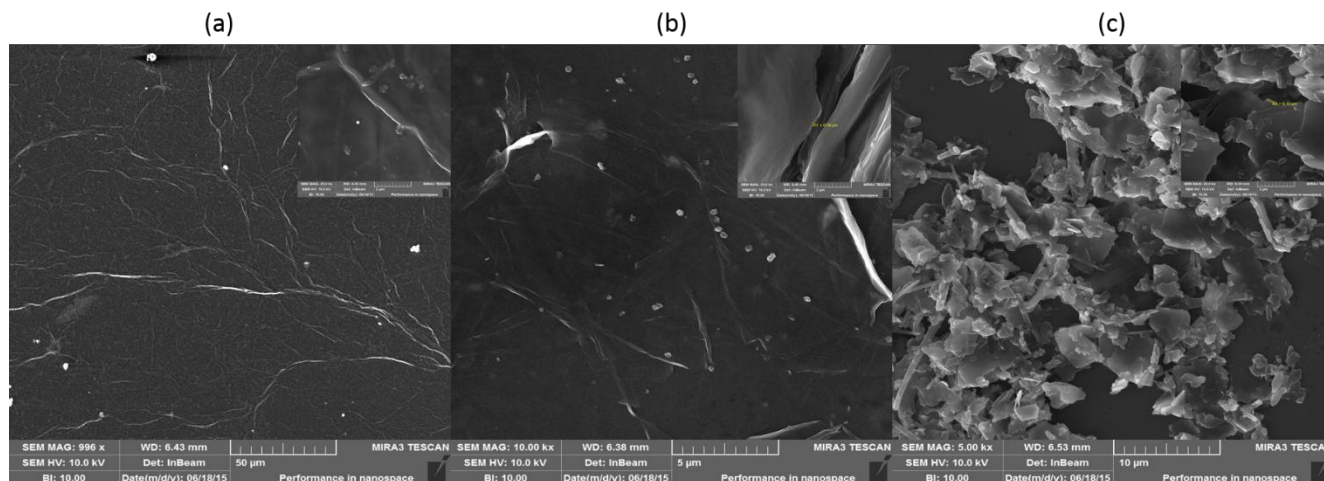


Figure 4. FESEM images of (a) GO, (b) GO-NH₂ and (c) GO-COOH showing morphological changes in GO before and after functionalization

For optical transparency, GO sheets were also visualized at 500 and 800 magnifications under optical microscope where few layered continuous and transparent GO sheets were observed (Figure5). The phenomenon behind the transparency of sheets was considered to be the stacking of layers of GO, contributing in greater thickness and causing increase in the reflection of light. In the case of few layers of GO (less thickness), the reflection is considered to be less, causing sheets to appear as transparent [31].

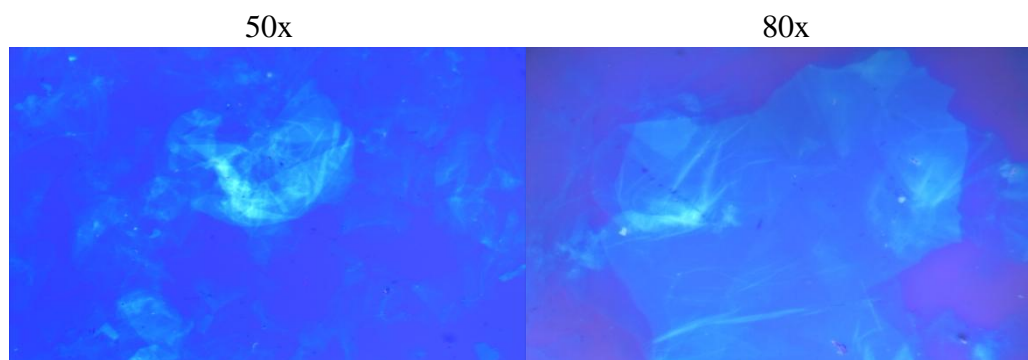


Figure 5. Optical microscope images of GO film on silicon substrate in the presence of polarized light under different magnifications, showing bright images for few layers of GO

Figure 6 shows the absorption spectra of GO, GO-COOH and GO-NH₂. The maximum absorption of GO was observed at 226nm whereas in the case of GO-NH₂ and GO-COOH the value of maximum absorption was 271nm and 330nm respectively. The reason behind this redshift is considered to be due to the extension in conjugation by incorporating benzene rings on the basal plan of GO. As discussed earlier, functionalization also caused partial reduction of graphene oxide thereby restoring conjugation (sp² hybridization), which might have increased the percolation pathways in the structure of graphene oxide [32].

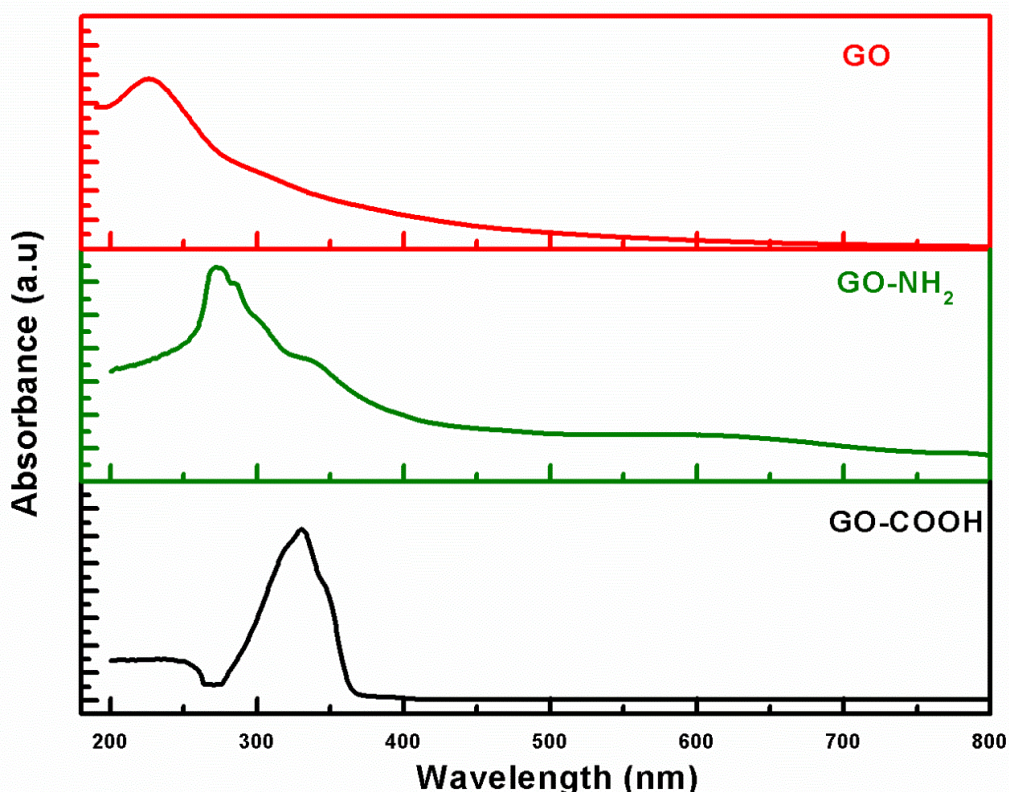


Figure 6. Absorption spectra of GO, GO-NH₂ and GO-COOH dispersions (0.5mg/ml) in DMF

In order to measure and compare the electrochemical performance of GO and functionalized GO, cyclic voltammetry (CV) was performed (Figure 7a). The samples for CV analysis were prepared by double Al electrode assembly method. Briefly, filter paper was soaked in 1M solution of sodium sulphate in water. Three drops of dispersions of samples were drop casted on the filter paper and it was sandwiched between two rectangular cut aluminum foils. The whole assembly was clamped between the two glass slides. The analysis was carried out at the scan rate of 100mV/s and the range of voltage was 0 to +1V. The CV curves showed that the value of current was maximum for GO-COOH which reached to a value of 2.2mA, whereas the minimum value of the current was observed in the case of pure GO i.e. ~0.4mA. Since the electrical conduction strongly depends on the delocalization of electronic orbitals, conjugation in the modified GO was extended due to the additional benzene rings in GO, enabling it to show higher current value [33]. In the case of GO-COOH considerable increase in the redox peak was observed, indicating its enhanced pseudo capacitive properties. Moreover, the

area of CV curves of GO-COOH and GO-NH₂ was found to be much higher in comparison to an earlier report on 9-anthracene carboxylic acid, indicating greater effect of conjugation in GO-COOH and GO-NH₂ leading to high conductivity [34].

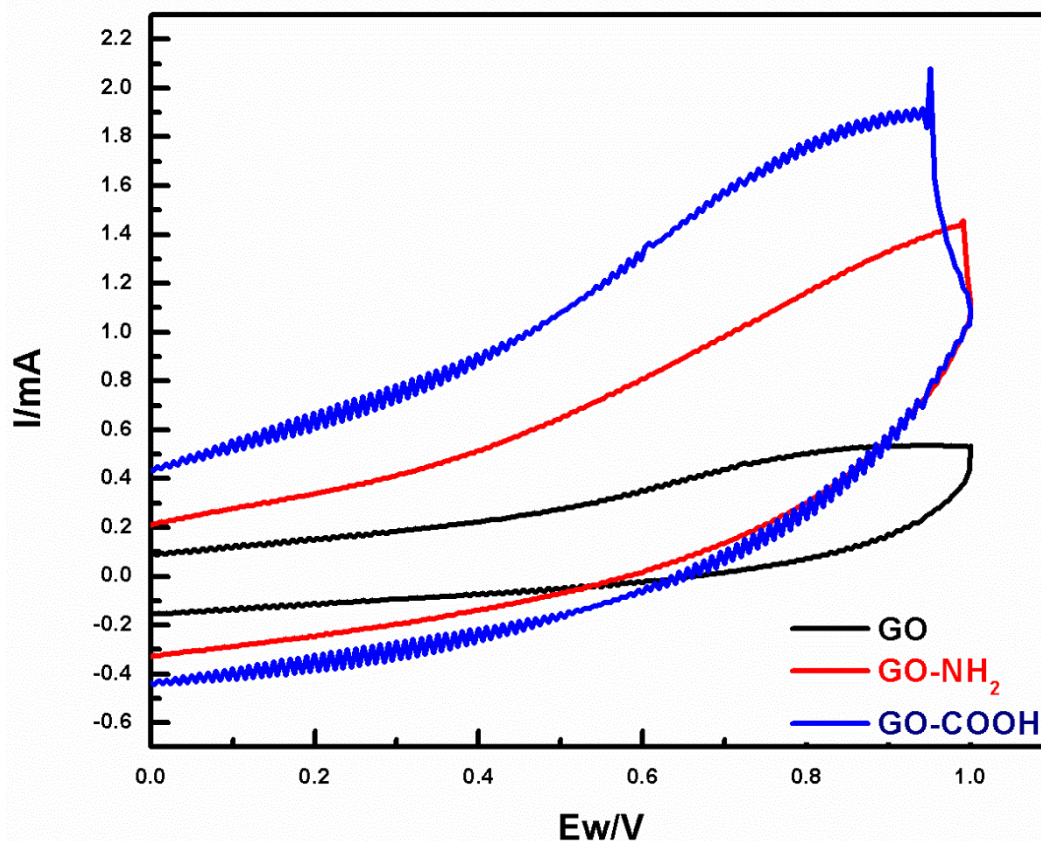


Figure 7. Cyclic Voltammetry curves of GO, GO-NH₂ and GO-COOH with a scan rate of 100mV/s

In order to investigate on the stability of curves and current values, five cycles of CV on samples were carried out (Figure 8). The obtained results were found to be promising regarding the stability of the current for multiple cycles since no significant change in the curves was observed (Figure 8). However, we could not find remarkable difference between the values for GO and functionalized GO.

Similarly, in order to study the stability in capacitance for the above samples, CV analysis was again carried out on five scan rates (Figure 9). Results of the analysis showed minor decrease in the capacitance as the scan rate was increased. Such small variation in the capacitance can be attributed to good charge propagation in the samples resulting in improved electrochemical properties. It can also be attributed to the fact that the capacitance current response is directly proportional to the time of analysis. As the scan rate increases, less time is provided to record the current response of the sample due to which low values of the current are obtained in comparison to the current values recorded in lower scan rates.

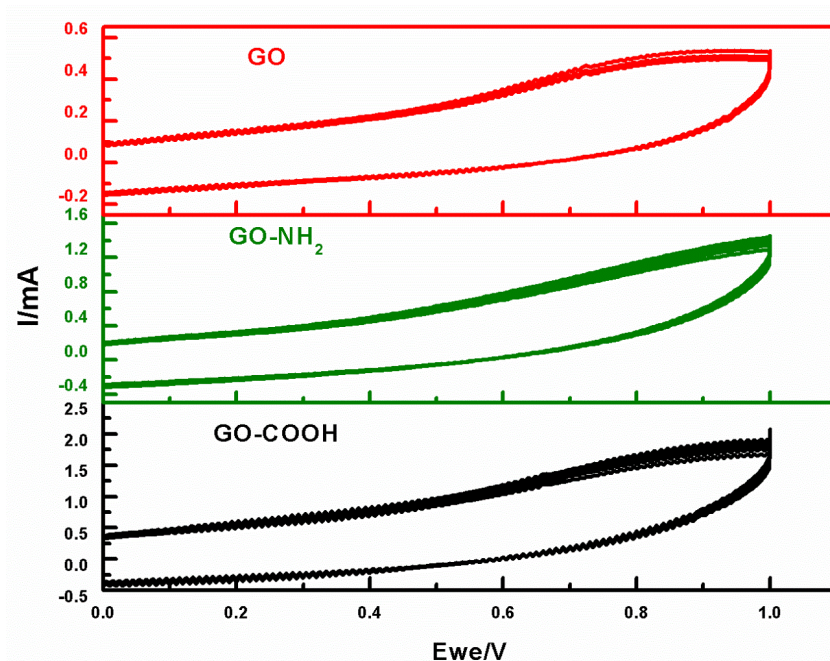


Figure 8. 5 Cycles of CV analysis of GO, GO-NH₂ and GO-COOH

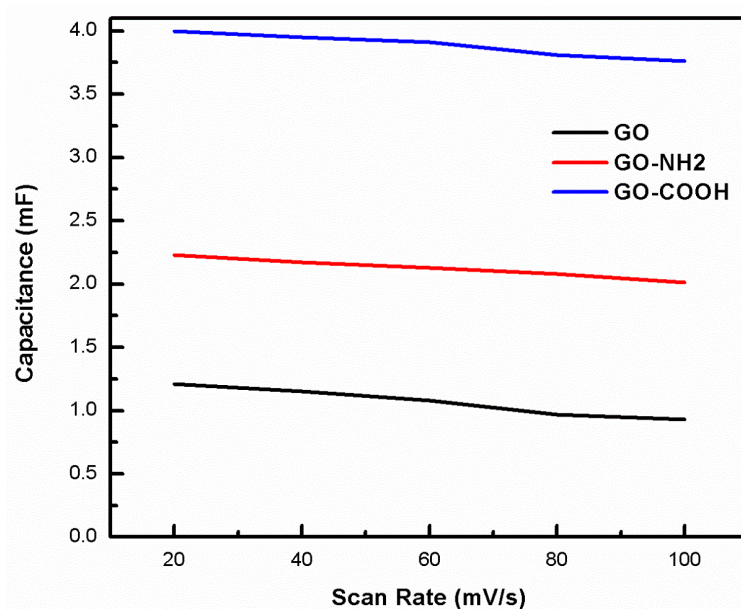


Figure 9. Capacitance Vs scan rate curves of GO and functionalized GO indicating the inverse relation between the capacitance and scan rate of CV analysis

The capacitance from the CV curves was calculated by dividing the current at 0V with the scan rate [35]. Results showed that the value of capacitance for GO-COOH was found to be 3.76 mF and for GO-NH₂ as 2.01mF while for pristine GO it was found to be 1/4th of the capacitance in comparison to GO-COOH. Such increase in the capacitance in functionalized GO, in particularly GO-COOH, could again be attributed to the extended conjugation as discussed earlier [36].

4. CONCLUSION

We have successfully prepared GO through chemical ex-foliation of graphite flakes and covalently attached organic molecules to the GO surface thereby extending the π -conjugation of the system. GO as well as chemically functionalized GO have been characterized through number of techniques such as FESEM, FTIR, UV-Vis, XRD and optical microscopy. Electrochemical performance of GO as well as functionalized GO was measured through CV analysis and compared. In comparison to GO, we have found significant increase in the capacitance with a factor of 2 and 4 in case of GO-NH₂ and GO-COOH respectively. Among other factors, such an increase in the capacitance could be attributed to extending conjugation through chemical functionalization of GO. Further work on such materials can lead to exploit them in energy storage applications such as supercapacitors and batteries.

ACKNOWLEDGEMENT

Z.H. gratefully acknowledges support from Prof. Dr. M. Mujahid, SCME–NUST for CV measurement through BioLogic VSP System purchased under NRPU project No. 20-1603/R&D/09/2236 funded by the Higher Education Commission (HEC) of Pakistan.

References

1. B. Dale, K. Dimitrios and B. Craig, *Journal of Power Sources*, 196(2011) 4873-4885.
2. S. Virendra, J. Daeha, Z. Lei, D. Soumen, K. Saiful and S. Sudipta, *Progress in Materials Science*, 56 (2011) 1178-1271.
3. J. Slonczewski and P. Weiss, *Phys. Rev.*, 109(1958) 272-279.
4. V. Luan, H. Tien, L. Hoa, N. Hien, O. Eun-Suok, C. JinSuk, K. Jung, C. Mook, K. Byung-Seon and H. Hyun, *Journal of Materials Chemistry A*, 1(2013) 208-211.
5. A. Balandin, S. Ghosh, W. Bao, I. Calizo, D. Teweldebrhan and F. Miao, *Nano Letters*, 8(2008) 902-907.
6. K. Novoselov, A. Geim, S. Morozov, D. Jiang, M. Katsnelson, I. Grigorieva, S. Dubonos and A. Firsov, *Nature*, 438(2005) 197-200.
7. K. Novoselov, A. Geim, S. Morozov, D. Jiang, Y. Zhang, S. Dubonos, I. Grigorieva and A. Firsov, *Science* 306(2004) 666-669.
8. C. Lee, X. Wei, J. Kysar and J. Hone, *Science* 321(2008) 385-388.
9. J. Wu, H. Becerril, Z. Bao, Z. Liu, Y. Chen and P. Peumans, *Appl. Phys. Lett.*, 92(2008) 263302-263305
10. X. Li, X. Wang, L. Zhang, S. Lee and H. Dai, *Science* 319(2008) 1229-1232.
11. K. Ritter and J. Lyding, *Nat Mater* 8(2009) 235-242.
12. D. Yu, E. Nagelli, R. Naik and L. Dai, *Angew. Chem., Int. Ed*, 50(2011) 6575-6578.
13. D. Yu, Y. Yang, M. Durstock, J. Baek and L. Dai, *ACS Nano*, 4(2010) 5633-5640.
14. L. Qu, Y. Liu, J. Baek and L. Dai, *ACS Nano* 4(2010) 1321-1326.
15. X. Xie, L. Qu, C. Zhou, Y. Li, J. Zhu, H. Bai, G. Shi and L. Dai, *ACS Nano*, 4(2010) 6050-6054.
16. Y. Zhang, Y. Tan, H. Stormer and P. Kim, *Nature*, 438(2005) 201-204.
17. K. Novoselov, Z. Jiang, Y. Zhang, S. Morozov, H. Stormer, U. Zeitler, J. Maan, G. Boebinger, P. Kim and A. Geim, *Science*, 315(2007) 1379.
18. B. Sharma and J. Ahn, *Solid State Electron.*, 89(2013) 177-188.

19. J. Paredes, S. Villar-Rodil, A. Marti'nez-Alonso and J. M. D. Tasco'n, *Langmuir*, 24(2008) 10560-10564.
20. K. Krishnamoorthy, M. Veerapandian, K. Yun and S. Kim, *Carbon*, 53(2013) 38-49.
21. T. Kuila, S. Bose, A. Mishra, P. Khanra, N. Kim and J. Lee, *Progress in Materials Science*, 57(2012) 1061-1105.
22. Z. Yan, H. Xue, K. Berning, Y. Lam, and C. Lee, *Appl. Mat. & Interfaces*, 6(2014) 22761-22768.
23. T. Kim, H. Lee, M. Stoller, D. Dreyer, C. Bielawski, R. Ruoff and K. Suh, *ACS Nano*, 5(2011) 436-441.
24. D. Marcano, D. Kosynkin, J. Berlin, A. Sinitskii, Z. Sun and A. Slesarev, *ACS Nano*, 4(2010) 4806-4814.
25. K. Krishnamoorthy, U. Navaneethaiyer, R. Mohan, J. Lee and S. Kim, *Appl. Nanosci.*, 2(2012) 119-126.
26. V. Gunasekaran, K. Kkrishnamoorthy, R. Mohan and S. Kim, *Mater. Chem. Phys.*, 132(2012) 29-33.
27. M. Cano, U. Khan, T. Sainsbury, A. O'Neill, Z. Wang, I. McGovern, W. Maser, A. Benito and J. Coleman, *Carbon*, 52(2013) 363-371.
28. J. Zheng, X. Ma, X. He, M. Gao, and G. Li., *Procedia Engineering*, 27(2012) 1478-1487.
29. I. Jung, J. Rhyee, J. Son, R. Ruoff and K. Rhee, *Nanotechnology*, 23(2012) 025708-025717.
30. Q. Zhang, Y. Li, Y. Feng and W. Feng, *Electrochimica Acta*, 90(2013) 95-100.
31. D. Li, M. Muller, S. Gilje, R. Kaner and G. Wallace, *Nature Nanotechnology*, 3(2008) 101-105.
32. T. Dadosh, Y. Gordin, R. Krahne, I. Khivrich, D. Mahalu, V. Frydman and J. Sperling, *Nature*, 436(2005) 677-680.
33. P. Khanra, M. Uddin, N. Kim, T. Kuila, S. Lee, J. Lee, *Rsc. Adv.*, 5(2015) 6443-6451.
34. D. Stoller, S. Park, Y. Zhu, Y. J. An, S. Ruoff, *Nano Letters*, 8(2008) 3498-3502.
35. I. Bersuker, *Electronic Structure and Properties of Transition Metal Compounds: 399 Introduction to the Theory*; 2nd ed.; wiley, United States of America, 2012.pp 238-371